To the Graduate Council:

I am submitting herewith a thesis written by David B. Simpson entitled "Incorporation of Consistent P_1 Theory Into DOT IV." I recommend that it be accepted in partial fulfillment of the requirements for the degree of Master of Science, with a major in Nuclear Engineering.

James C. Robinson

James C. Robinson, Major Professor

We have read this thesis
and recommend its acceptance:

George Flanagan

P F Pasqua

R L Doldo Jr

Accepted for the Council:

L Evans Roth

Vice Chancellor
Graduate Studies and Research

cop. 2

INCORPORATION OF CONSISTENT P_1 THEORY INTO DOT IV

A Thesis

Presented for the

Master of Science

Degree

The University of Tennessee, Knoxville

David B. Simpson

June 1977

1324149

ACKNOWLEDGEMENTS

This work was performed in the Neutron Physics Division of Oak Ridge National Laboratory which is operated by Union Carbide Corporation for the Energy Research and Development Administration. W. A. Rhoades was the project leader for DOT IV development and his cooperation in implementing the consistent P_1 approximation is greatly appreciated.

ABSTRACT

In this work, a P_1 difference formulation is developed for implementation into the DOT IV computer program. Linearly anisotropic sources and scattering cross sections are included in the formulation. Auxiliary functions are introduced to yield equations which are stable with respect to round off errors and to allow implementation of certain boundary conditions in a natural way.

To check the correctness of the method, a problem was chosen for which the solution should compare favorably with a diffusion solution. The problem also illustrated the absence of ray effects in the P_1 approximation. As expected, the P_1 solution agreed well with the diffusion solution.

A hydrogenous medium problem was analyzed to illustrate the importance of linearly anisotropic scattering. Use of P_1 scattering cross sections for hydrogen produced a k-effective in the P_1 approximation about 20 percent lower than those obtained from diffusion approximations. This difference was confirmed by comparing an S_2P_1 to an S_2P_0 calculation.

The convergence rate for the P_1 approximation was found to be much less than an unaccelerated alternating direction diffusion theory calculation. The slow rate of convergence for some problems makes the P_1 solution scheme presently implemented in DOT IV an unattractive option.

TABLE OF CONTENTS

CHAPTER		PAGE
I.	INTRODUCTION	1
	General Remarks	1
	Scope and Organization	3
II.	CONSISTENT P_1 SOLUTION SCHEME	4
	Theoretical Model	4
	Numerical Model	12
	Iterative Scheme	20
	Boundary Conditions	21
	Limitations	22
III.	NUMERICAL RESULTS	25
	Ray Effect Problem	25
	Hydrogenous Medium Problem	28
IV.	SUMMARY AND RECOMMENDATIONS	35
LIST OF REFERENCES		37
APPENDIX		39
VITA		42

LIST OF FIGURES

FIGURE PAGE

1. Coordinates for Particle Scattering in Rectangular Geometry 7
2. Cylindrical Coordinate System 8
3. Comparison of Right Edge Scalar Flux in a Pure Absorber Between S_2, Diffusion, and P_1 Approximations 27
4. Cylindrical Geometry Representation of the Hydrogenous Medium Problem 29
5. Plot of Hydrogenous Medium Left Boundary Scalar Fluxes . . 33
6. Plot of Hydrogenous Medium Bottom Boundary Scalar Fluxes 34

CHAPTER I

INTRODUCTION

General Remarks

The central problem of neutron transport calculations is to determine the neutron flux throughout a given region of space having a specified composition of materials. The neutron flux distribution is found by solving the Boltzman transport equation. However, exact analytic solutions may be obtained for a limited class of problems only and it is necessary, in general, to adopt approximate methods for solving the transport equation.

The method of discrete ordinates is possibly the most powerful and generally used method of solving the transport equation. Several computer programs have been developed which employ this method.[1] DOT III is a computer program which uses the method of discrete ordinates to solve radiation transport problems in two spatial dimensions.[2]

In the discrete ordinates approximation, the angular distribution of the neutron flux is evaluated in a number of discrete directions. Greater accuracy of the solution may be attained by choosing more directions. Accurate solutions to deep penetration shielding problems as well as those where streaming may occur require a large number of directions to represent the angular distribution of the neutron flux. Also, a large number of spatial mesh points are required to adequately approximate the spatial distribution of the neutron flux in problems where steep flux gradients occur.

Until recently, two-dimensional transport solutions to problems possessing these characteristics required computers having large storage capacity. A new computer program, named DOT IV, is presently being developed[3] and will solve larger problems with less core memory. DOT IV is able to solve large shielding problems by retaining only a row of space mesh data in fast memory at a time. Other features include allowing radial space mesh and directional quadrature to vary with axial position, a module for producing a diffusion theory solution, a module for producing a P_1 theory solution, and several other features required for efficient interfacing with other installations and/or machines.

Transport solutions are required if either very precise solutions are desired or the logarithmic gradient of the neutron flux is on the order of or larger than an inverse mean free path over locally significant portions of the phase space.[4] However, use of the diffusion theory method will, in many situations, provide a good approximation to the transport solution, and diffusion theory is commonly used for preliminary design calculations.

Diffusion theory is derived from the P_1 spherical harmonics approximation. This derivation includes the approximation of the anisotropic scattering contribution to the energy transfer. If sources are isotropic, diffusion theory and P_1 theory are equivalent for one-speed problems. For practical applications, scattering is seldom isotropic in the laboratory system and the equivalence between multigroup diffusion and multigroup P_1 theories is consequently destroyed. Therefore, a multigroup P_1 solution

would generally be more accurate compared with a multigroup diffusion solution.

Scope and Organization

It is the objective of this work to develop a technique for obtaining numerical solutions to be multigroup P_1 equations and to incorporate this technique into the DOT IV computer program. To accomplish this objective, difference equations adaptable to either X-Y, R-Z, or R-θ geometries were derived from the P_1 approximation and an alternating direction sweep suggested by Carlson[5] was chosen for solving these equations.

In the following chapter, the derivation of the three two-dimensional P_1 equations chosen for implementation as well as the numerical approach chosen for solving these equations is presented in detail. Results are presented in Chapter III for a few calculations performed to evaluate the usefulness and limitations of this method. In Chapter IV, conclusions resulting from these calculations are presented along with recommendations for extending this approach.

CHAPTER II

CONSISTENT P_1 SOLUTION SCHEME

Theoretical Model

The energy dependent transport equation for general geometry may be written[6]

$$\vec{\Omega}\cdot\vec{\nabla}\Phi(\vec{r},\vec{\Omega},E) + \sigma(\vec{r},E)\ \Phi(\vec{r},\vec{\Omega},E) = \int_{E'}\int_{\vec{\Omega}'}\sigma_s(\vec{r},E')$$

$$f(\vec{r};\ \vec{\Omega}',E'\rightarrow\vec{\Omega},E)\ \Phi(\vec{r},\vec{\Omega}',E')\ d\vec{\Omega}'dE' + S(\vec{r},\vec{\Omega},E). \qquad (2.1)$$

The total source, $S(\vec{r},\vec{\Omega},E)$, is composed of fission and extraneous sources, and is given by

$$S(\vec{r},\vec{\Omega},E) = \frac{1}{4\pi}\chi(E)\int_{E'}\nu\sigma_f(\vec{r},E')\int_{\vec{\Omega}'}\Phi(\vec{r},\vec{\Omega}',E')\ d\vec{\Omega}'dE'$$

$$+ Q(\vec{r},\vec{\Omega},E). \qquad (2.2)$$

The symbols in Equations (2.1) and (2.2) are defined as follows:

$\Phi(\vec{r},\vec{\Omega},E)$ = the angular flux distribution as a function of position $\vec{r}$, direction $\vec{\Omega}$, and energy E,

$\sigma(\vec{r},E)$ = the macroscopic total cross section,

$\sigma_s(\vec{r},E')f(\vec{r};\vec{\Omega}',E'\rightarrow\vec{\Omega},E)$ = the probability that a scattering collision will transfer a neutron from $\vec{\Omega}',E'$ to $\vec{\Omega},E$,

$\chi(E)$ = the energy distribution of fission neutrons,

$\nu\sigma_f(\vec{r},E')$ = the probability that ν neutrons will result from fission, and

$Q(\vec{r},\vec{\Omega},E)$ = the extraneous angular source distribution.

If the angular variation of the transfer probability is assumed to depend only on the angle between the initial and final directions, i.e., $\vec{\Omega}'\cdot\vec{\Omega}(\equiv\mu_o)$, then the transfer probability may be expanded in Legendre polynomials to obtain

$$\sigma_s(\vec{r},E')\ f(\vec{r};\vec{\Omega}',E'\to\vec{\Omega},E) = \sigma_s(\vec{r},E')\ f(\vec{r};E'\to E,\ \mu_o)$$

$$= \sum_{\ell=0}^{\infty} \frac{2\ell+1}{4\pi}\ \sigma_{s,\ell}(\vec{r},E'\to E)\ P_\ell(\mu_o), \qquad (2.3)$$

where the expansion coefficients, $\sigma_\ell(\vec{r},E'\to E)$, are given by

$$\sigma_{s,\ell}(\vec{r},E'\to E) = 2\pi \int_{-1}^{1} \sigma_s(\vec{r},E')f(\vec{r};E'\to E,\ \mu_o)\ P_\ell(\mu_o)\ d\mu_o.$$

Inserting Equation (2.3) into Equation (2.1) yields

$$\vec{\Omega}\cdot\vec{\nabla}\Phi + \sigma\Phi = \frac{1}{4\pi} \sum_{\ell=0}^{\infty} (2\ell+1) \int_{E'} \sigma_{s,\ell}(\vec{r},E'\to E) \int_{\Omega'} P_\ell(\mu_o)\Phi' d\vec{\Omega}' dE' + S, \qquad (2.4)$$

where arguments have been omitted for brevity.

According to the addition theorem of Legendre polynomials,[6] $P_\ell(\mu_o)$ may be expressed as

$$P_\ell(\mu_o) = P_\ell(\mu)\ P_\ell(\mu') + 2 \sum_{m=1}^{\ell} \frac{(\ell-m)!}{(\ell+m)!} P_\ell^m(\mu)\ P_\ell^m(\mu')$$

$$[\cos m\phi \cos m\phi' + \sin m\phi \sin m\phi'], \qquad (2.5)$$

where μ, μ', ϕ, and ϕ' are defined in Figure 1 for rectangular coordinates. A prime represents the initial direction value, μ is the cosine of the polar angle, and ϕ is the azimuthal angle. The coordinate system used for cylindrical geometry is given in Figure 2. As shown in Figure 2, μ is the cosine of the polar angle and ϕ is the azimuthal angle. Since cylindrical coordinates are orthogonal, and the definitions for μ, μ', ϕ, and ϕ' are consistent with their definitions in rectangular coordinates, Equation (2.5) is also valid for cylindrical coordinates.

Using Equation (2.5), Equation (2.4) may be rewritten as

$$\vec{\Omega}\cdot\vec{\nabla}\Phi + \sigma\Phi = \frac{1}{4\pi}\sum_{\ell=0}^{\infty}(2\ell+1)\int_{E'}\sigma_{s,\ell}(\vec{r},E'\to E)\int_{\vec{\Omega}'} P_\ell(\mu)\,P_\ell(\mu')\,\Phi'\,d\vec{\Omega}'\,dE' + S$$

$$+\frac{1}{2\pi}\sum_{\ell=1}^{\infty}\sum_{m=1}^{\ell}(2\ell+1)\frac{(\ell-m)!}{(\ell+m)!}\int_{E'}\sigma_{s,\ell}(\vec{r},E'\to E)\int_{\vec{\Omega}'} P_\ell^m(\mu)P_\ell^m(\mu')$$

$$\times\,[\cos m\phi\cos m\phi' + \sin m\phi\sin m\phi']\,\Phi'\,d\vec{\Omega}'\,dE'. \qquad (2.6)$$

Consistent with a first order spherical harmonic expansion, as shown in Appendix A, the angular flux may be represented by

$$\Phi(\vec{r},\vec{\Omega},E) = \frac{1}{4\pi}\,[\phi(\vec{r},E) + 3\vec{\Omega}\cdot\vec{J}(\vec{r},E)], \qquad (2.7)$$

where $\phi(\vec{r},E)$ is the scalar flux, defined by

$$\phi(\vec{r},E) = \int_{\vec{\Omega}}\Phi(\vec{r},\vec{\Omega},E)\,d\vec{\Omega},$$

ORNL-DWG 77-9096

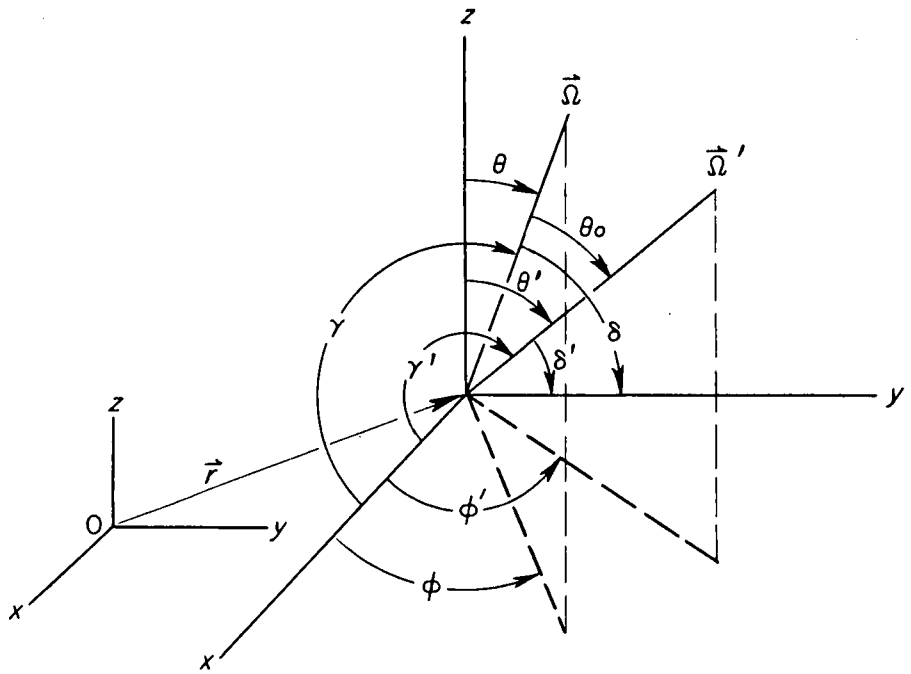

$$\Omega_z = \vec{\Omega} \cdot \hat{e}_z = \cos\ \theta \equiv \mu$$
$$\Omega_x = \vec{\Omega} \cdot \hat{e}_x = \cos\ \gamma = \sin\ \theta\ \cos\ \phi = \sqrt{1-\mu^2}\ \cos\ \phi$$
$$\Omega_y = \vec{\Omega} \cdot \hat{e}_y = \cos\ \delta = \sin\ \theta\ \sin\ \phi = \sqrt{1-\mu^2}\ \sin\ \phi$$
$$\Omega'_z = \vec{\Omega}' \cdot \hat{e}_z = \cos\ \theta' = \mu'$$
$$\Omega'_x = \vec{\Omega}' \cdot \hat{e}_x = \cos\ \gamma' = \sin\ \theta'\ \cos\ \phi' = \sqrt{1-\mu'^2}\ \cos\ \phi'$$
$$\Omega'_y = \vec{\Omega} \cdot \hat{e}_y = \cos\ \delta' = \sin\ \theta'\ \sin\ \phi' = \sqrt{1-\mu'^2}\ \sin\ \phi'$$
$$\vec{\Omega}' \cdot \vec{\Omega} = \cos\ \theta_0 \equiv \mu_0$$

Figure 1. Coordinates for Particle Scattering in Rectangular Geometry.

ORNL-DWG 77-9097

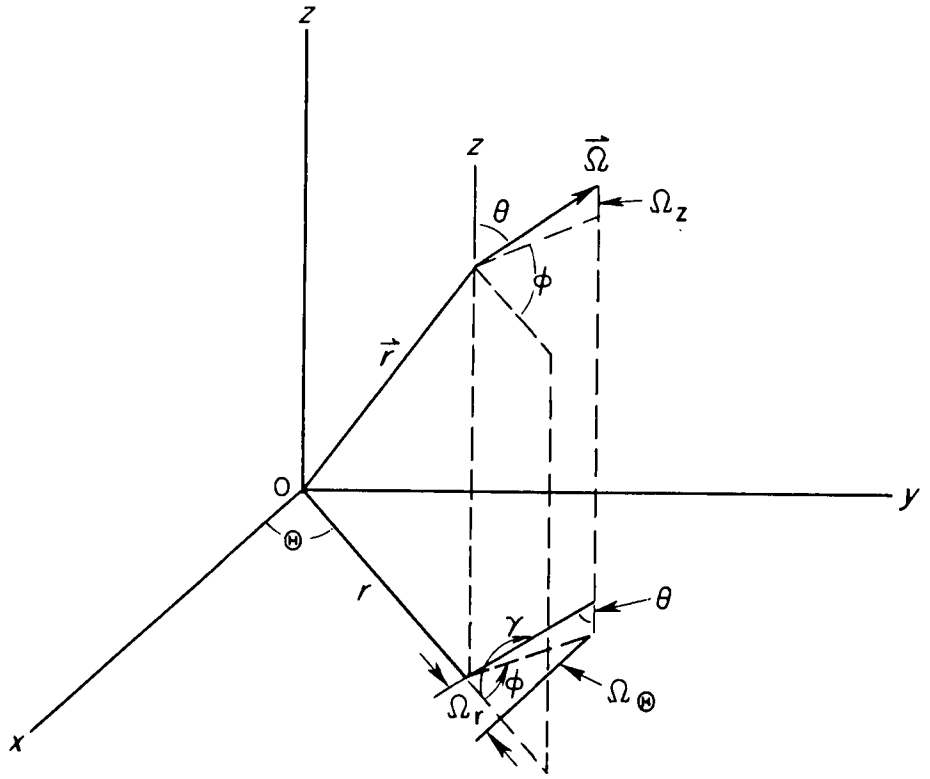

$$\Omega_z = \vec{\Omega} \cdot \hat{e}_z = \cos\theta \equiv \mu$$

$$\Omega_r = \vec{\Omega} \cdot \hat{e}_r = \cos\gamma = \sin\theta \cos\phi = \sqrt{1-\mu^2} \cos\phi$$

$$\Omega_\Theta = \vec{\Omega} \cdot \hat{e}_\Theta$$

$$= (1-\Omega_r^2-\Omega_z^2)^{1/2} = \sin\theta \sin\phi = \sqrt{1-\mu^2} \sin\phi$$

Figure 2. Cylindrical Coordinate System.

and $\vec{J}(\vec{r},E)$ is the current, defined by

$$\vec{J}(\vec{r},E) = \int_{\vec{\Omega}} \vec{\Omega}\phi(\vec{r},\vec{\Omega},E)\, d\vec{\Omega}.$$

In a similar manner, the angular distribution of the source may be expanded as

$$S(\vec{r},\vec{\Omega},E) = \frac{1}{4\pi}\,[S_o(\vec{r},E) + 3\vec{\Omega}\cdot\vec{S}_1(\vec{r},E)], \tag{2.8}$$

where the expansion coefficients are defined as

$$S_o(\vec{r},E) = \int_{\vec{\Omega}} S(\vec{r},\vec{\Omega},E)\, d\vec{\Omega}, \text{ and}$$

$$\vec{S}_1(\vec{r},E) = \int_{\vec{\Omega}} \vec{\Omega}\, S(\vec{r},\vec{\Omega},E)\, d\vec{\Omega}.$$

Inserting Equations (2.7) and (2.8) into the left side of Equation (2.6) yields, after multiplying by 4π and omitting arguments,

$$\vec{\Omega}\cdot\vec{\nabla}[\phi+3\vec{\Omega}\cdot\vec{J}] + \sigma[\phi+3\vec{\Omega}\cdot\vec{J}] = S_o + 3\vec{\Omega}\cdot\vec{S}_1$$

$$+ \sum_{\ell=0}^{\infty} (2\ell+1) \int_{E'} \sigma_{s,\ell}(\vec{r},E'\to E) \int_{\Omega'} P_\ell(\mu)\, P_\ell(\mu')\, \Phi' d\vec{\Omega}' dE'$$

$$+ 2 \sum_{\ell=1}^{\infty} \sum_{m=1}^{\ell} (2\ell+1) \frac{(\ell-m)!}{(\ell+m)!} \int_{E'} \sigma_{s,\ell}(\vec{r},E'\to E) \int_{\Omega'} P_\ell^m(\mu) P_\ell^m(\mu')$$

$$\times [\cos m\phi \cos m\phi' + \sin m\phi \sin m\phi']\, \Phi'\, d\vec{\Omega}' dE'. \tag{2.9}$$

Using the orthogonality of the spherical harmonics,[6] the integrals over $\vec{\Omega}'$ on the right side of Equation (2.9) are zero except those for which $\ell=0$ or $\ell=1$, since Equations (2.7) and (2.8) are

equivalent to a first-order spherical harmonic expansion. Hence, Equation (2.9) becomes

$$\vec{\Omega}\cdot\vec{\nabla}(\phi+3\vec{\Omega}\cdot\vec{J}) + \sigma(\phi+3\vec{\Omega}\cdot\vec{J}) = S_o + 3\vec{\Omega}\cdot\vec{S}_1$$

$$+ \int_{E'} \sigma_{s,o}(\vec{r},E'\to E) \int_{\Omega'} \Phi' d\Omega' dE'$$

$$+ 3\int_{E'} \sigma_{s,1}(\vec{r},E'\to E) \int_{\Omega'} [\mu\mu' + \sqrt{1-\mu^2}\cos\phi\sqrt{1-\mu'^2}\cos\phi'$$

$$+ \sqrt{1-\mu^2}\sin\phi\sqrt{1-\mu'^2}\sin\phi'] \Phi' d\vec{\Omega}' dE'.$$

In obtaining the above expression, use was made of the definition $P_1^1(\mu) \equiv \sqrt{1-\mu^2} = \sin\theta$. Recognizing the term in brackets above to be $\vec{\Omega}\cdot\vec{\Omega}'$, the above equation reduces to

$$\vec{\Omega}\cdot\vec{\nabla}(\phi+3\vec{\Omega}\cdot\vec{J}) + \sigma(\phi+3\vec{\Omega}\cdot\vec{J}) = S_o + 3\vec{\Omega}\cdot\vec{S}_1$$

$$+ \int_{E'} \sigma_{s,o}(\vec{r},E'\to E) \int_{\vec{\Omega}'} \Phi' d\vec{\Omega}' dE' + 3\int_{E'} \sigma_{s,1}(\vec{r},E'\to E)$$

$$\vec{\Omega} \cdot \int_{\vec{\Omega}'} \vec{\Omega}'\Phi' d\vec{\Omega}' dE'. \qquad (2.10)$$

Equation (2.10) may be rewritten, making use of previous definitions, as

$$\vec{\Omega}\cdot\vec{\nabla}(\phi+3\vec{\Omega}\cdot\vec{J}) + \sigma(\phi+3\vec{\Omega}\cdot\vec{J}) = S_o + 3\vec{\Omega}\cdot\vec{S}_1$$

$$+ \int_{E'} \sigma_{s,o}(\vec{r},E'\to E)\ \phi' dE' + 3\int_{E'} \sigma_{s,1}(\vec{r},E'\to E)\ \vec{\Omega}\cdot\vec{J}' dE'. \qquad (2.11)$$

Integration of Equation (2.11) over $\vec{\Omega}$ yields

$$\vec{\nabla}\cdot\vec{J}(\vec{r},E) + \sigma(\vec{r},E)\ \phi(\vec{r},E) = S_o(\vec{r},E) + \int_{E'} \sigma_{s,o}(\vec{r},E'\to E)\ \phi(\vec{r},E')\ dE'.$$

(2.12)

After multiplying by $\vec{\Omega}$ and then integrating, Equation (2.11) becomes

$$\vec{\nabla}\phi(\vec{r},E) + 3\sigma(\vec{r},E)\,\vec{J}(\vec{r},E) =$$

$$3\,\vec{S}_1(\vec{r},E) + 3\int_{E'} \sigma_{s,1}(\vec{r},E'\to E)\,\vec{J}(\vec{r},E')\,dE'. \qquad (2.13)$$

Equations (2.12) and (2.13) are the P_1 approximation to the energy dependent transport equation in general geometry.

A multigroup scheme is generally employed to approximate the energy dependence of the scalar flux and current. By definition, a group is an energy interval having boundaries E_g and E_{g-1}. The integral over E' may then be expressed as a sum of integrals over all the energy groups, i.e., $\int dE' = \sum_{g'} \int_{E_{g'}}^{E_{g'-1}} dE'$. If Equations (2.12) and (2.13) are integrated over an energy group, the result is

$$\vec{\nabla}\cdot\vec{J}_g(\vec{r}) + \sigma_{o,g}(\vec{r})\,\phi_g(\vec{r}) = \sum_{g'=1}^{G} \sigma_{o,g'\to g}(\vec{r})\,\phi_{g'}(\vec{r}) + S_{o,g}(\vec{r}), \qquad (2.14)$$

and

$$\vec{\nabla}\phi_g(\vec{r}) + 3\sigma_{1,g}(\vec{r})\,\vec{J}_g(\vec{r}) = 3\sum_{g'=1}^{G} \sigma_{1,g'\to g}(\vec{r})\,\vec{J}_{g'}(\vec{r}) + 3\,\vec{S}_{1,g}(\vec{r}), \qquad (2.15)$$

$$g = 1, 2, \ldots G.$$

In deriving Equations (2.14) and (2.15), use was made of the following definitions:

$$\phi_g(\vec{r}) \equiv \int_{E_g}^{E_{g-1}} \phi(\vec{r},E)\,dE,$$

$$\vec{J}_g(\vec{r}) \equiv \int_{E_g}^{E_{g-1}} \vec{J}(\vec{r},E)\,dE,$$

$$S_{o,g}(\vec{r}) \equiv \int_{E_g}^{E_{g-1}} S_0(\vec{r},E)\,dE,$$

$$\vec{S}_{1,g}(\vec{r}) \equiv \int_{E_g}^{E_{g-1}} \vec{S}_1(\vec{r},E)\, dE\,,$$

$$\sigma_{o,g}(\vec{r}) \equiv \frac{\int_{E_g}^{E_{g-1}} \sigma(\vec{r},E)\, \phi(\vec{r},E)\, dE}{\int_{E_g}^{E_{g-1}} \phi(\vec{r},E)\, dE}\,,$$

$$\sigma_{1,g}(\vec{r}) \equiv \frac{\int_{E_g}^{E_{g-1}} \sigma(\vec{r},E)\, \vec{J}(\vec{r},E)\, dE}{\int_{E_g}^{E_{g-1}} \vec{J}(\vec{r},E)\, dE}\,,$$

$$\sigma_{o,g'\to g}(\vec{r}) \equiv \frac{\int_{E_{g'}}^{E_{g'-1}} \phi(\vec{r},E') \int_{E_g}^{E_{g-1}} \sigma_{s,o}(\vec{r},E'\to E)\, dE\, dE'}{\int_{E_{g'}}^{E_{g'-1}} \phi(\vec{r},E')\, dE'}\,, \text{ and}$$

$$\sigma_{1,g'\to g}(\vec{r}) \equiv \frac{\int_{E_{g'}}^{E_{g'-1}} \vec{J}(\vec{r},E') \int_{E_g}^{E_{g-1}} \sigma_{s,1}(\vec{r},E'\to E)\, dE\, dE'}{\int_{E_{g'}}^{E_{g'-1}} \vec{J}(\vec{r},E')\, dE'}\,.$$

With the exception that $\sigma_{o,g}(\vec{r})$ is used in place of $\sigma_{1,g}(\vec{r})$, Equations (2.14) and (2.15) serve as the analytic basis for obtaining an approximate numerical solution via the consistent P_1 solution scheme implemented in DOT IV.

Numerical Model

To obtain a numerical solution to Equations (2.14) and (2.15), the spatial dependence of the flux and currents is represented by the value of each at a set of discrete space points. This is

accomplished by defining the domain of $\vec{r}$ by a set of nonoverlapping mesh cells from which approximate difference equations may be derived. If the domain of the radial component of $\vec{r}$ is specified by IM intervals having arbitrary width, and the domain of the axial component of $\vec{r}$ is specified by JM intervals having arbitrary width, IM times JM mesh cells are defined by the intersection of the orthogonal surfaces which pass through each interval boundary.

The volume of a cell is designated by $V_{i+1/2,\ j+1/2}$, where the centered subscripts locate the center of the cell. A subscript i denotes the left endpoint and a subscript i+1/2 the midpoint of the ith radial interval. Similar subscripts, with j replacing i, are used for the axial intervals. The area of the cell face coinciding with the (constant radial) coordinate surface which passes through the left endpoint of the i-th radial interval is denoted by A_i, and the area of the cell face which coincides with the (constant axial) coordinate surface which passes through the bottom endpoint of the j-th axial interval is denoted by B_j. DOT IV is used to obtain specified solutions for systems having geometrical representation in either of three two-dimensional geometries -- X-Y, R-Z, or R-θ. Expressions for the cell volume and areas of the cell faces are given in Table I for each of these geometries.

In deriving difference equations for a mesh cell from which a numerical solution may be obtained, frequent use is made of the mean value theorem for integrals. As a result, the difference equations for a mesh cell involve average values of the flux and currents for the volume and for the cell faces. These average values

TABLE I

AREA AND VOLUME ELEMENTS FOR X-Y, R-Z, and R-Θ GEOMETRIES

	X-Y	R-Z[1]	R-Θ[1,2]
A_i	ΔY_j	$2\pi r_i \Delta Z_j$	$2\pi r_i \Delta \Theta_j$
B_j	ΔX_i	$2\pi \bar{r}_i \Delta Z_j$	Δr_i
V_{ij}	$\Delta X_i \Delta Y_j$	$2\pi \bar{r}_i \Delta r_i \Delta Z_j$	$2\pi \bar{r}_i \Delta r_i \Delta \Theta_j$

[1] $\bar{r} \equiv \frac{1}{2}(r_i + r_{i+1})$.

[2] Θ is specified in revolutions.

are approximated by the value at the center of the volume or cell face, depending on the domain of integration. Appropriate centered subscripts, as mentioned above, are appended to the flux and currents to denote these midpoint values. In order to simplify the notation, however, centered subscripts, although understood, will be omitted. Thus, the flux at the cell center is designated as ϕ and the flux at the midpoint of a cell face is designated as ϕ_i, ϕ_{i+1}, ϕ_j, or ϕ_{j+1}, depending on which cell face is involved. Since the current is a vector quantity, it is specified by a radial direction component designated as I and an axial direction component designated as J. Subscripts are appended to these components in the same manner they are appended to the flux.

Difference equations are derived by replacing $\sigma_{l,g}(\vec{r})$ with $\sigma_{o,g}(\vec{r})$ in Equations (2.14) and (2.15) and then integrating the resulting equations over the volume of the mesh cell. Equation (2.14) becomes, after performing these operations and making use of the mean value and Gauss divergence theorems,

$$A_{i+1} I_{i+1} - A_i I_i + B_{j+1} J_{j+1} - B_j J_j + \sigma_o V\phi = VS_o + \sum_{g'=1}^{G} \sigma_{o_{g'\to g}} \phi_{g'} V. \tag{2.16}$$

Equation (2.15) is a vector equation. For equality, corresponding vector components on each side must be equal. After utilizing the mean value theorem and performing the above operations, Equation (2.15) becomes, for the radial direction components,

$$A(\phi_{i+1}-\phi_i) + 3\sigma_o VI = 3VS_I + \sum_{g'=1}^{G} (3\sigma_{1_{g'\to g}}) I_{g'} V , \tag{2.17}$$

and, for the axial direction components,

$$B(\phi_{j+1}-\phi_j) + 3\sigma_o VJ = 3VS_J + \sum_{g'=1}^{G} (3\sigma_{1_{g'\to g}}) J_{g'}V, \qquad (2.18)$$

where $A \equiv 1/2\ (A_i+A_{i+1})$ and $B \equiv 1/2\ (B_j+B_{j+1})$. To obtain Equation (2.17), the mean value for the radial component of the flux gradient was approximated by a central difference involving the fluxes at the midpoints of the appropriate cell faces. Subsequent multiplication by the cell volume yields an expression which may be written in the form of the first term in Equation (2.17). Equation (2.18) was derived in a similar manner. S_I represents the radial component of $\vec{S}_1$ and S_J the axial component. Upon subtracting $\sigma_{o_{g\to g}} \phi_g V$ from each side, Equation (2.16) may be written

$$A_{i+1}I_{i+1} - A_iI_i + B_{j+1}J_{j+1} - B_jJ_j + \sigma^r V\phi = VS_o + \sum_{g'\neq g} \sigma_{o_{g'\to g}} \phi_{g'}V, \qquad (2.19)$$

where $\sigma^r \equiv \sigma_o - \sigma_{o_{g\to g}}$. After subtracting $3\sigma_{1_{g\to g}} I_g V$ from each side, Equation (2.17) becomes

$$A(\phi_{i+1}-\phi_i) + 3\sigma^{tr}VI = 3VS_I + \sum_{g'\neq g} (3\sigma_{1_{g'\to g}}) I_{g'}V, \qquad (2.20)$$

where $\sigma^{tr} \equiv \sigma_o - \sigma_{1_{g\to g}}$. In a similar manner, Equation (2.18) may be written as

$$B(\phi_{j+1}-\phi_j) + 3\sigma^{tr}VJ = 3VS_J + \sum_{g'\neq g} (3\sigma_{1_{g'\to g}}) J_{g'}V. \qquad (2.21)$$

Equations (2.19), (2.20), and (2.21) involve three terms in I, three terms in J, and five terms in ϕ. One term in I, one term in J, and two terms in ϕ are known from boundary conditions or from a calculation in an adjoining cell. A difference scheme is then required in order to solve these equations. The difference scheme used is the following:

$$2\phi = \phi_i + \phi_{i+1} = \phi_j + \phi_{j+1},$$

$$2I = I_i + I_{i+1}, \text{ and}$$

$$2J = J_j + J_{j+1}.$$

Substitution of these difference relations yields, for the radial direction,

$$A_{i+1}I_{i+1} - A_iI_i + 1/2\ \sigma^r V(\phi_{i+1}+\phi_i) = VS_o + \sum_{g'\neq g} \sigma_{o_{g'\to g}} \phi_{g'} V$$

$$- (B_{j+1}J_{j+1} - B_jJ_j), \tag{2.22}$$

$$A(\phi_{i+1}-\phi_i) + \frac{3}{2}\sigma^{tr} V(I_{i+1}+I_i) = 3VS_I + \sum_{g'\neq g} (3\sigma_{1_{g'\to g}})\, I_{g'} V, \tag{2.23}$$

and

$$B_{j+1}J_{j+1} - B_jJ_j + \frac{1}{2} V\sigma^r(\phi_{j+1}+\phi_j) = VS_o + \sum_{g'\neq g} \sigma_{o_{g'\to g}} \phi_{g'} V$$

$$- (A_{i+1}I_{i+1} - A_iI_i), \tag{2.24}$$

$$B(\phi_{j+1}-\phi_j) + \frac{3}{2} V\sigma^{tr}(J_{j+1}+J_j) = 3VS_J + \sum_{g'\neq g} (3\sigma_{1_{g'\to g}})\, J_{g'} V \tag{2.25}$$

for the axial direction. Equations (2.22) through (2.25) are then solved by an iterative scheme analogous to the alternating direction implicit (ADI) iterative procedure[7] used to invert diffusion theory matrices.

In order to circumvent round off problems and facilitate the application of right and top boundary conditions, four auxiliary functions are introduced and used to set up a general relationship between incoming and outgoing neutron flow. This procedure is called the reflection principle by Carlson,[5] although it should properly be referred to as Schmidt's method.[8] In effect, it is postulated that

$$I_i = p_i\phi_i - q_i, \tag{2.26}$$

$$I_{i+1} = p_{i+1}\phi_{i+1} - q_{i+1}, \tag{2.27}$$

$$J_j = t_j\phi_j - U_j, \tag{2.28}$$

and

$$J_{j+1} = t_{j+1}\phi_{j+1} - U_{j+1}. \tag{2.29}$$

If Equation (2.27) is substituted into Equation (2.22) and (2.23), and the expression for ϕ_{i+1} obtained from Equation (2.23) after modification is substituted into the modified Equation (2.22), the resulting expression may be reduced to the form of Equation (2.26). Upon equating coefficients, it is found that

$$p_i = \frac{2\tilde{\sigma}_o A + (AA_{i+1} + \tilde{\sigma}_o\tilde{\sigma}_1)\, p_{i+1}}{AA_i + \tilde{\sigma}_o\tilde{\sigma}_1 + 2\tilde{\sigma}_1 A p_{i+1}}, \tag{2.30}$$

$$q_i = \frac{(p_{i+1}\tilde{\sigma}_1+A)[\tilde{S}_o-(B_{j+1}J_{j+1}-B_jJ_j)]-(\tilde{\sigma}_o+p_{i+1}A_{i+1})S_a+(AA_{i+1}-\tilde{\sigma}_o\tilde{\sigma}_1)q_{i+1}}{AA_i+\tilde{\sigma}_o\tilde{\sigma}_1+2\tilde{\sigma}_1Ap_{i+1}}, \tag{2.31}$$

where

$$\tilde{\sigma}_o \equiv \frac{1}{2} V\sigma^r,$$

$$\tilde{\sigma}_1 \equiv \frac{3}{2} V\sigma^{tr},$$

$$\tilde{S}_o \equiv VS_o + \sum_{g'\neq g} \sigma_{o_{g'\to g}} \phi_{g'}V,$$

and

$$S_a \equiv 3VS_I + \sum_{g'\neq g} (3\sigma_{1_{g'\to g}}) I_{g'}V.$$

Using Equations (2.24), (2.25), (2.28), and (2.29), it is found using a similar procedure that

$$t_j = \frac{2\tilde{\sigma}_oB+(BB_{j+1}+\tilde{\sigma}_o\tilde{\sigma}_1)t_{j+1}}{BB_j+\tilde{\sigma}_o\tilde{\sigma}_1+2\tilde{\sigma}_1B\ t_{j+1}}, \tag{2.32}$$

$$U_j = \frac{(B+\tilde{\sigma}_1\ t_{j+1})[\tilde{S}_o-(A_{i+1}I_{i+1}-A_iI_i)]-(\tilde{\sigma}_o+B_{j+1}t_{j+1})S_b+(BB_{j+1}-\tilde{\sigma}_o\tilde{\sigma}_1)U_{j+1}}{BB_j+\tilde{\sigma}_o\tilde{\sigma}_1+2\tilde{\sigma}_1Bt_{j+1}}, \tag{2.33}$$

where $S_b \equiv 3VS_J + \sum_{g'\neq g} (3\sigma_{1_{g'\to g}}) J_{g'}V$. Substituting Equations (2.26) and (2.27) into (2.22) yields, after simplification,

$$\phi_{i+1} = \frac{(A_ip_i-\tilde{\sigma}_o)\phi_i-(B_{j+1}J_{j+1}-B_jJ_j)+(A_{i+1}q_{i+1}-A_iq_i)+\tilde{S}_o}{A_{i+1}p_{i+1}+\tilde{\sigma}_o}. \tag{2.34}$$

Substituting Equations (2.28) and (2.29) into (2.24) yields

$$\phi_{j+1} = \frac{(B_j t_j - \tilde{\sigma}_o)\phi_j - (A_{i+1} I_{i+1} - A_i I_i) + (B_{j+1} U_{j+1} - B_j U_j) + \tilde{S}_o}{B_{j+1} t_{j+1} + \tilde{\sigma}_o}. \qquad (2.35)$$

Iterative Scheme

Since the P_1 equations do not involve a self-scatter source term, no iteration is needed in solving for the flux in any row or column of the mesh if correct values of the transverse direction currents are known. This is usually not the case however, and iterations are required in order to obtain a solution. For each row of the mesh, values for p and q are obtained using Equations (2.30) and (2.31) and marching inward from the outer boundary. Values for the flux and radial direction current are then computed using Equations (2.34) and (2.26) and marching outward. Values for the axial direction currents calculated from the previous axial sweep are used when obtaining a solution from the radial sweep. Using the values of the radial direction currents just calculated, each column of the mesh is swept from top to bottom to calculate values for t and U using Equations (2.32) and (2.33). Values for the flux and axial direction current are then obtained from Equations (2.35) and (2.28) upon marching from bottom to top. One iteration is defined to be a radial sweep followed by an axial sweep of the mesh. Iterations are continued, up to a specified limit, until the maximum relative difference in point flux values between the radial and axial sweeps is less than a specified criterion.

Boundary Conditions

The boundary conditions used are of the albedo type. An albedo is the fraction of the current leaving a boundary which returns; i.e., $J^- = \gamma J^+$ where γ is the albedo. For a non-reentrant boundary, the albedo is zero and for a reflected boundary, the albedo is unity. Using the consistent P_1 approximation, it may easily be shown that $J = \frac{1}{2}\left(\frac{1-\gamma}{1+\gamma}\right)\phi$ if no boundary angular source is present. If an extraneous boundary angular source is present, the boundary current is specified as $J = \frac{1}{2}\left(\frac{1-\gamma}{1+\gamma}\right)\phi - 2Q$, where Q is the inward directed flow due to the extraneous source. Since DOT IV is used primarily in obtaining solutions using a discrete ordinates algorithm, a boundary condition compatible with a Mark boundary condition was chosen for implementation. If a two-dimensional S_2 Gaussian quadrature is used where each weight is equal to 0.25 and the abscissas are all the possible combinations of $(\pm\sqrt{3/3}, \pm\sqrt{3/3})$, it may be shown that $J = \frac{\sqrt{3}}{3}\left(\frac{1-\gamma}{1+\gamma}\right)\phi - 2Q$.

If γ_R is the albedo at the right boundary, then $p_{IM+1} = \frac{\sqrt{3}}{3}\left(\frac{1-\gamma_R}{1+\gamma_R}\right)$ and $q_{IM+1} = 2Q_R$. If γ_T is the albedo at the top boundary, then $t_{JM+1} = \frac{\sqrt{3}}{3}\left(\frac{1-\gamma_T}{1+\gamma_T}\right)$ and $U_{JM+1} = 2Q_T$. If γ_L is the albedo at the left boundary, then $I = -\frac{\sqrt{3}}{3}\left(\frac{1-\gamma_L}{1+\gamma_L}\right)\phi + 2Q_L$. Using the relation $I = p\phi - q$, it is found that

$$\phi_L = \frac{q_1 + 2Q_L}{P_1 + \frac{\sqrt{3}}{3}\left(\frac{1-\gamma_L}{1+\gamma_L}\right)}$$

In a similar manner, it is found that

$$\phi_B = \frac{U_1 + 2\,Q_B}{t_1 + \frac{\sqrt{3}}{3}\left(\frac{1-\gamma_B}{1+\gamma_B}\right)}$$

where γ_B is the albedo for the bottom boundary. To correspond with a Marshak boundary condition, an albedo of 0.0718 may be specified, and an albedo equal to 0.1030 may be specified to correspond with an extrapolated end point boundary condition with extrapolation distance equal to $0.71\ \lambda_{tr}$.

Limitations

It is possible that the right hand side of Equation (2.22) could be negative for certain phase space cells. For these cells, an auxiliary difference equation was used in which the transverse leakage was taken to the left hand side and treated as a removal to ensure a positive source. Equation (2.22) then becomes

$$A_{i+1}I_{i+1} - A_iI_i + \frac{1}{2}V\sigma^x(\phi_{i+1}+\phi_i) = VS_o + \sum_{g'\neq g}\sigma_{o_{g'\to g}}\phi_{g'}V, \qquad (2.36)$$

where $\sigma^x \equiv \sigma^r + \frac{B(J_{j+1}-J_j)}{V\phi^p}$. The superscript p implies that a value for the scalar flux from the previous iteration is used. Use of this previous iterate flux alters the balance property of Equation (2.22). A rescaling operation is then required to restore this balance.

The rescaling operation used after the i-direction sweep employs a single scale factor f_i to provide a global balance for the mesh.

This scale factor is given by

$$f_i = \frac{SORTG - \sum_{RHS\geq 0} B(J_{j+1}-J_j)}{SORTG - \sum_{RHS\geq 0} B(J_{j+1}-J_j) - \sum_{RHS<0} \frac{B(J_{j+1}-J_j)}{\phi^p}(\phi - \phi^p)}, \quad (2.37)$$

where the summation of the extraneous and downscatter (isotropic component) sources for all mesh cells is denoted by SORTG. The symbol $\sum_{RHS\geq 0}$ implies summation over only those mesh cells for which the right hand side of Equation (2.22) is positive, and the symbol $\sum_{RHS<0}$ implies only those cells for which the right hand side is negative.

In a similar manner, an alternative difference equation is used when the right hand side of Equation (2.24) is negative and is given by

$$B_{j+1}J_{j+1} - B_jJ_j + \frac{1}{2}V\sigma^y(\phi_{j+1}+\phi_j) = VS_o + \sum_{g'\neq g} \sigma_{o\,g'\to g}\phi_{g'}V, \quad (2.38)$$

where $\sigma^y \equiv \sigma^r + \frac{A_{i+1}I_{i+1} - A_iI_i}{V\phi^p}$. The scale factor used after the j-direction sweep is given by

$$f_j = \frac{SORTG - \sum_{RHS\geq 0} [A_{i+1}I_{i+1} - A_iI_i]}{SORTG - \sum_{RHS\geq 0} [A_{i+1}I_{i+1} - A_iI_i] - \sum_{RHS\geq 0} \frac{A_{i+1}I_{i+1} - A_iI_i}{\phi^p}(\phi - \phi^p)}. \quad (2.39)$$

One important limitation of this method is that a sufficiently fine mesh must be chosen so that values of the auxiliary variables q and U, as well as values for the flux, calculated from their corresponding recursion relations are positive. Negative values of the flux are incorrect on physical grounds, but are easily obtained in

regions where a flux gradient is present if a sufficiently fine mesh spacing is not used.

In order to show that values for q (and U) must be positive, the albedo concept is employed. Using an equation similar to that used at the left boundary, the value for q at mesh boundary i is given by

$$q_i = \left(p_i + \frac{\sqrt{3}}{3}\frac{1-\gamma_i}{1+\gamma_i}\right)\phi_i ,$$

where γ_i is the albedo at that mesh boundary and $0 \leq \gamma_i \leq 1$. It is easily seen from Equation (2.30) that values of p_i are positive. Since values of the scalar flux should be positive, and since $0 \leq \gamma_i \leq 1$, it is apparent that values for q should be positive. However, Equation (2.31) does not guarantee that q will remain positive. Due to the nonlinear form of this recursion relation, a suitable fixup for a negative q is not obvious.

CHAPTER III

NUMERICAL RESULTS

In order to evaluate the consistent P_1 formulation developed in Chapter II, page 4, two test problems were analyzed by a collection of routines which have been implemented in the DOT IV computer program and which utilize the solution scheme for this formulation. Comparative results were obtained from diffusion and discrete ordinates routines also implemented in DOT IV. The two test problems were chosen to illustrate the advantages, as well as the limitations, of the formulation. The purpose of this chapter is to present and discuss the results from these calculations.

Ray Effect Problem

Distortions in the scalar flux in certain discrete ordinates calculations, called ray effects, are due to the discretization of the angular variable in the streaming term of the transport equation. Since particles are restricted to travel in straight lines, streaming contributions to the flux at a given point in the medium are limited to sources which are intercepted by the directions of the discrete set. Spherical harmonic solutions do not possess ray effects.

A problem suggested by William H. Reed[9] was chosen to illustrate the absence of ray effects in a solution obtained from the consistent P_1 formulation. Comparative solutions were obtained from a diffusion theory calculation and an S_2 discrete ordinates calculation. A geometrical description, including cross sections

and boundary conditions, is presented in Figure 3 along with a plot of the scalar flux near the right boundary obtained from each calculation. The S_2 results were obtained using a Gaussian quadrature, with weights equal to one-fourth and abscissas given by all possible combinations of $(\pm \sqrt{3/3}, \pm \sqrt{3/3})$, and a weighted difference formulation. S_2 compatible boundary conditions were used for the P_1 solution.

Since the problem consisted of a localized source in a pure absorber, the S_2 results exhibit the expected ray effect due to the low order quadrature. The diffusion and P_1 results are qualitatively correct. Since the source was isotropic and absorption was the only type of interaction involved, values of the flux at points several mean free paths from the right and top boundaries should be approximately the same for each calculation. This was observed to be true, the small differences presumably due to a second-order difference approximation compared with a first-order.

The objective of this test case was to show that ray effects are not present in a P_1 solution and that a P_1 approximation is equivalent to a diffusion approximation for isotropic scattering and sources. Problems involving isolated sources in weakly scattering media, however, are those for which transport solutions are required to obtain accurate results. Therefore, a discrete ordinates calculation with many directions would have provided a better result.

The exact solution was obtained by a numerical integration of

$$\phi(3.9,Y) = \int_{-1.2}^{1.2} \int_{-1.2}^{1.2} \frac{S}{2\pi d} \int_{0}^{\pi/2} e^{-d(\sec \theta)} \, d\theta \, dx' \, dy',$$

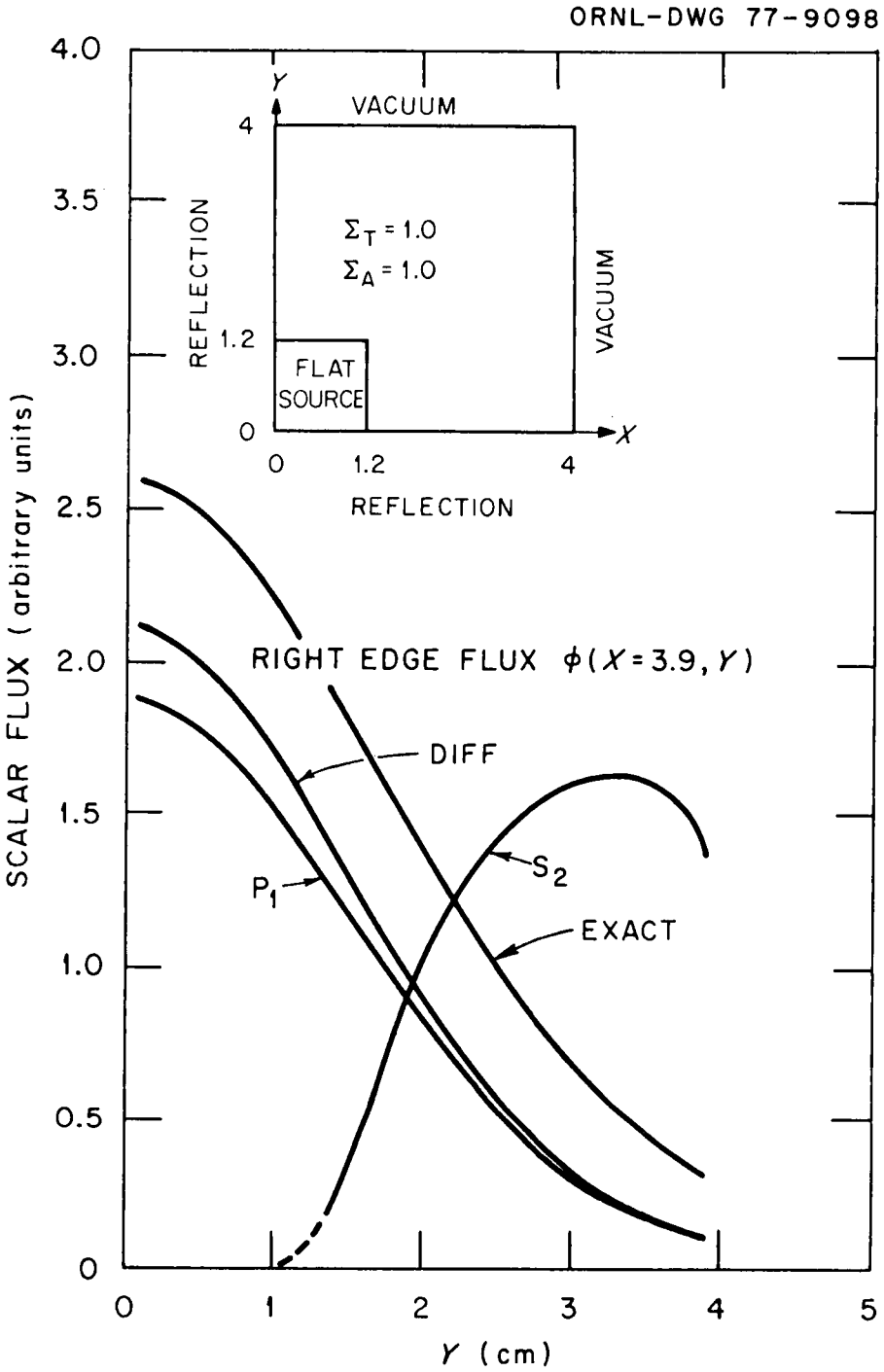

Figure 3. Comparison of Right Edge Scalar Flux in a Pure Absorber Between S_2, Diffusion, and P_1 Approximations.

where

$$S = 1/1.44 \text{ and } d = [(3.9 - x')^2 + (y - y')^2]^{1/2}.$$

It was observed from these calculations that the diffusion approximation required slightly less computer time per iteration than the P_1 approximation. However, the P_1 approximation provides values for three unknowns per mesh cell while diffusion theory provides only one. Using an IBM 360 Model 91 computer, diffusion theory averaged about 0.7 million mesh cell calculations per minute and P_1 theory about 0.5 million. Although convergence rates are problem dependent, the P_1 approximation required 361 iterations and the diffusion approximation with no acceleration required 87 iterations before the maximum pointwise relative flux change per iteration was less than 10^{-4}.

Hydrogenous Medium Problem

The second test case was chosen to illustrate the importance of linearly anisotropic scattering. This importance is best emphasized in hydrogenous media. The model chosen represents a ten inch diameter aluminum cylinder containing an aqueous solution of uranyl fluoride, UO_2F_2, submerged in water. The aqueous uranyl fluoride had a hydrogen to U-235 ratio equal to 52.9 and was 93.4 percent enriched. The geometrical representation is shown in Figure 4 and the atom densities of each nuclide in each region is presented in Table II. The Hansen-Roach sixteen group cross sections[10] were used in the analysis.

In order to evaluate the utility of the consistent P_1 approximation, calculations for this hydrogenous medium were also performed using diffusion theory with no within-group correction to σ^t, using

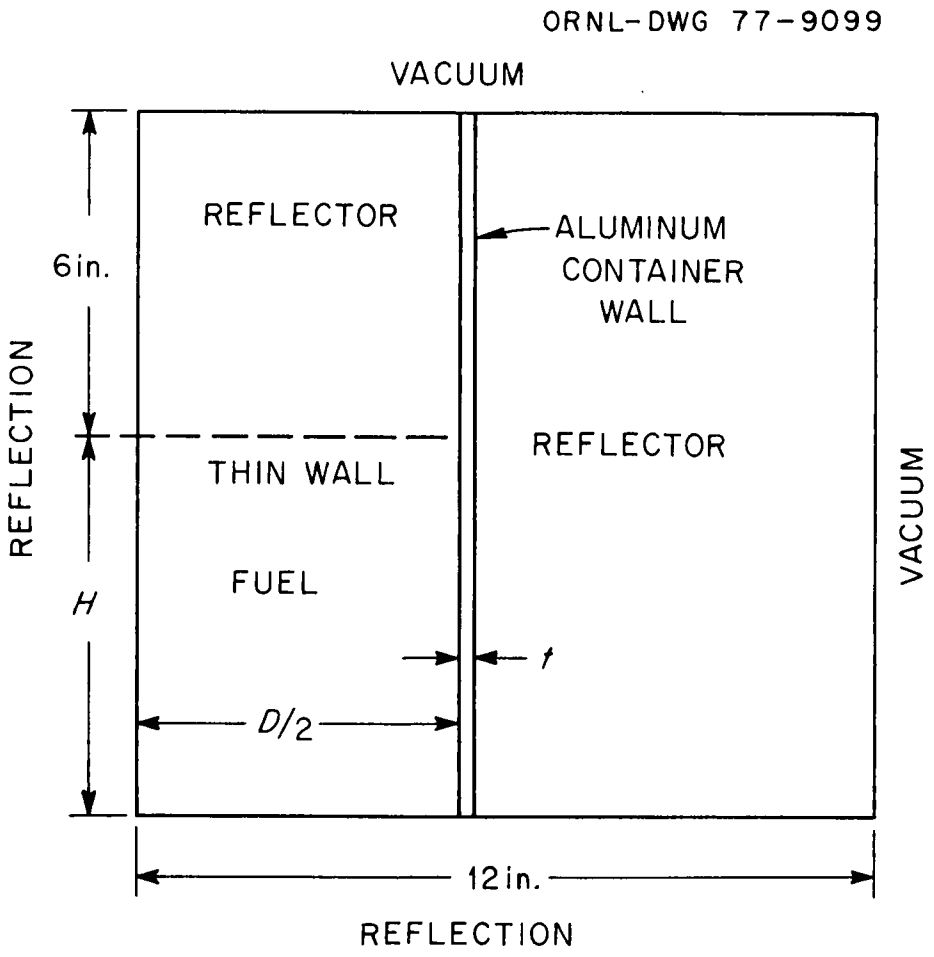

D = 10 in. (25.4 cm)

t = $1/16$ in. (0.15875 cm)

H = 13.4 cm

Figure 4. Cylindrical Geometry Representation of the Hydrogenous Medium Problem

TABLE II

HYDROGENOUS MEDIUM ATOMIC DENSITIES BY NUCLIDE BY REGION

	Atomic Density*		
Nuclide	Core	Reflector	Container Wall
U-235	1.1748-3	---	---
U-238	8.3014-5	---	---
F	2.5156-3	---	---
H	6.2147-2	6.6922-2	---
O	3.3589-2	3.3461-2	---
Al	---	---	6.02-2

*Densities are expressed in units of 10^{-24} atoms/cm^3.

diffusion theory with transport-corrected total cross sections, using an S_2 discrete ordinates approximation having isotropic and linearly anisotropic scattering, and using an S_4 discrete ordinates approximation with linearly anisotropic scattering. Due to the approximations involved, the eigenvalue resulting from the S_4P_1 calculation was judged to be the most accurate, and a comparison of calculated eigenvalues and the corresponding percent deviation from the S_4P_1 eigenvalue is given in Table III.

Upon reviewing Table III, it is apparent that the downscatter to lower groups from the linear component of the anisotropic scattering is very important for this problem. For an S_2 calculation, the difference in k_{eff} between isotropic and linearly anisotropic scattering is approximately 20 percent. With this in mind, it is seen that uncorrected diffusion theory gives a value of k_{eff} approximately 24 percent higher than the consistent P_1 k_{eff}. Using transport-corrected cross sections, the diffusion theory k_{eff} is still approximately 21 percent higher than the consistent P_1 k_{eff}. The difference in eigenvalues between diffusion theory and P_1 theory compares favorably with the difference in eigenvalues between an S_2P_0 and an S_2P_1 calculation.

A plot of the left boundary scalar flux for group one and for group sixteen obtained from the consistent P_1 approximation is presented in Figure 5. A plot of the bottom boundary scalar flux for group one and for group sixteen is presented in Figure 6. A plot of the corresponding values obtained from the S_4P_1 calculation. The consistent P_1 calculation accurately predicts the peak of the thermal flux near the reflector interface and illustrates an exponential decay of the fast flux inside the reflector.

TABLE III

COMPARISON OF CALCULATED EIGENVALUES FOR THE HYDROGENOUS MEDIUM USING DIFFERENT APPROXIMATIONS

Model	K	% DIF[a]
Consistent P_1	1.0183	-4.3
S_4P_1	1.0638	---
S_2P_1	1.0887	2.3
S_2P_0	1.3115	23.3
Diffusion[b]	1.2629	18.7
Diffusion[c]	1.2383	16.4

[a]Based on the k for the S_4P_1 being correct, i.e.,

$$\% \text{ DIF} = \frac{K - 1.0638}{1.0638} \times 100.$$

[b]No correction to σ^t was made.

[c]σ^t was corrected by the linear within-group scattering cross section.

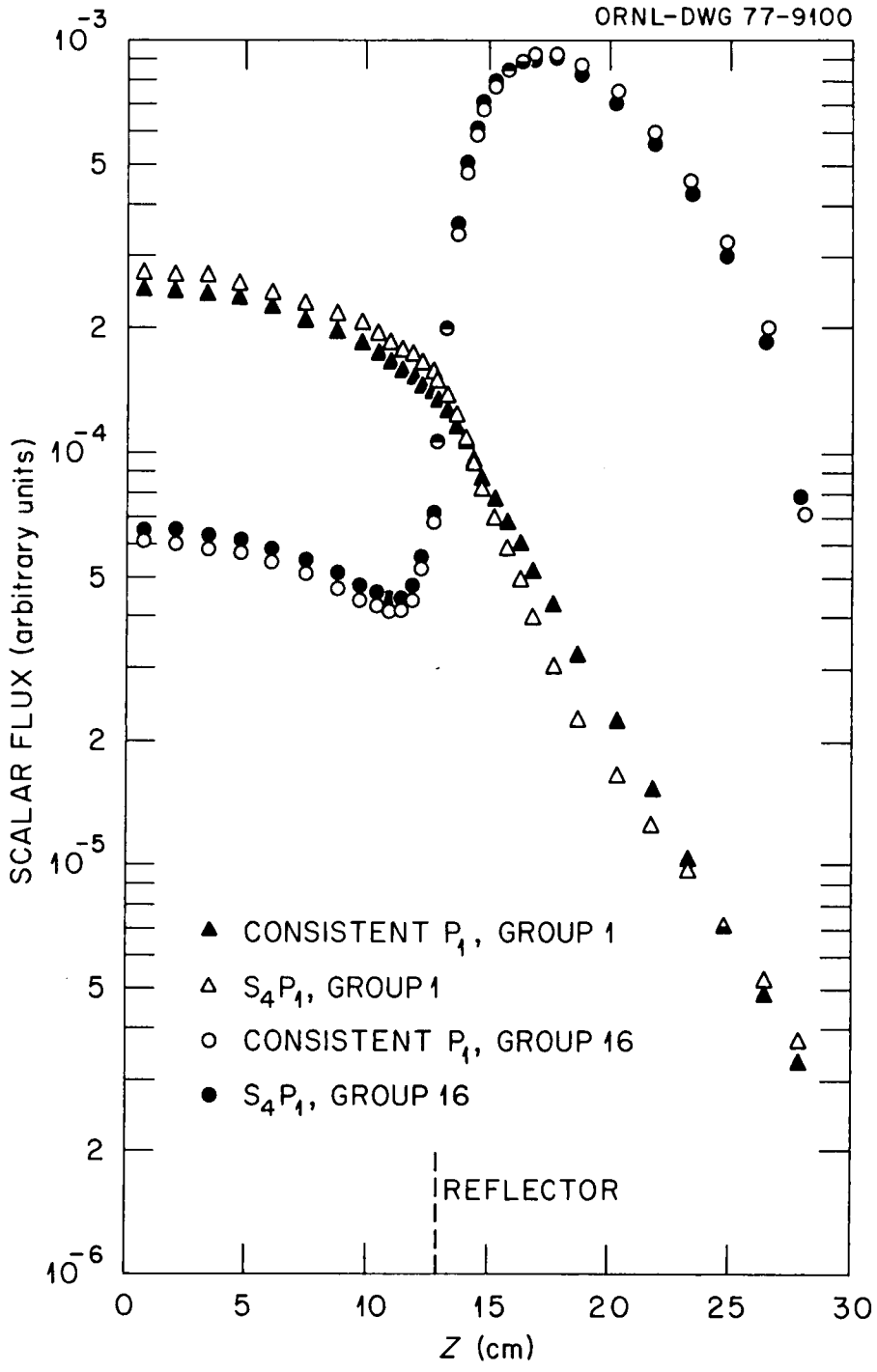

Figure 5. Plot of Hydrogenous Medium Left Boundary Scalar Fluxes.

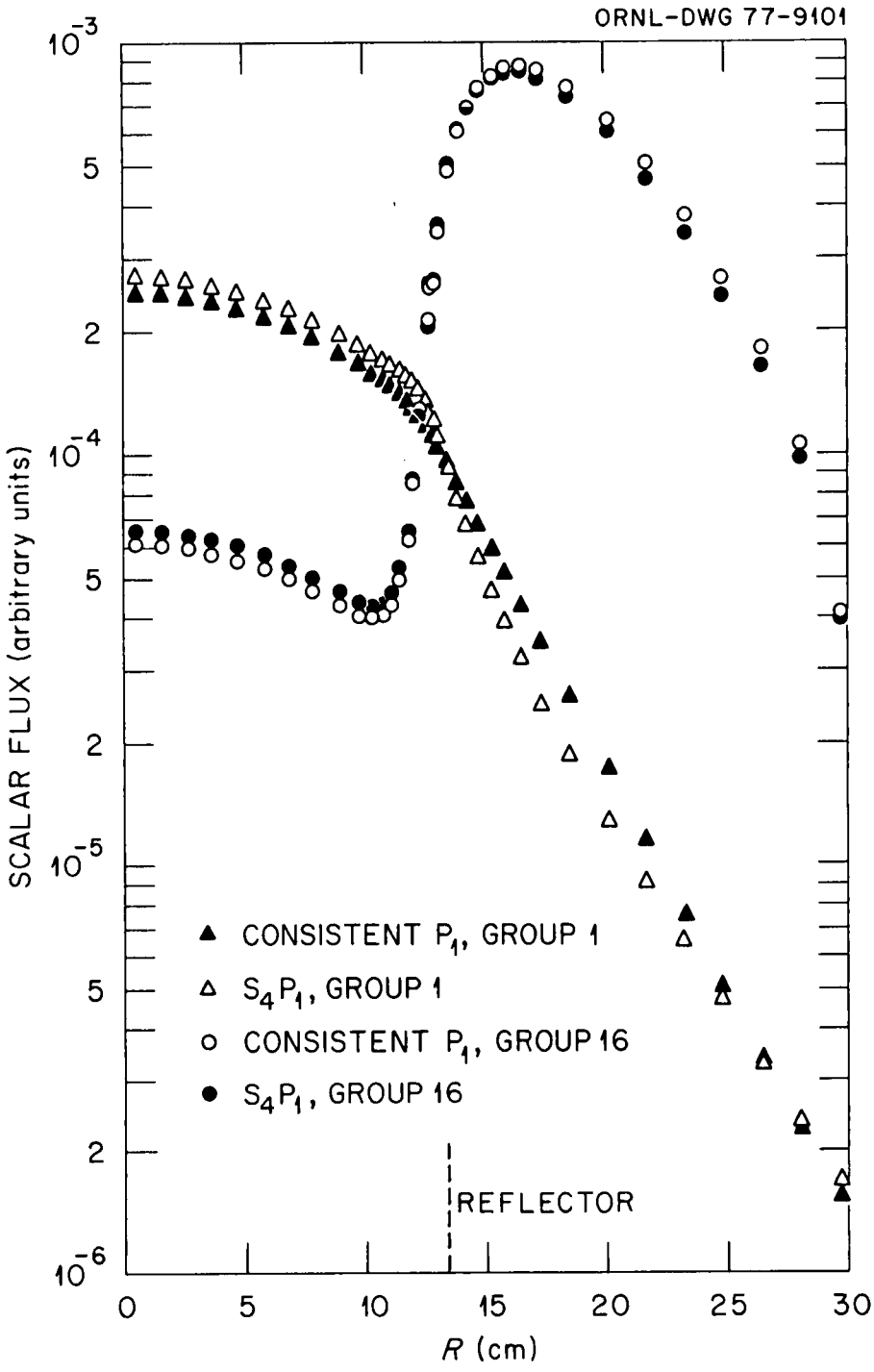

Figure 6. Plot of Hydrogenous Medium Bottom Boundary Scalar Fluxes.

CHAPTER IV

SUMMARY AND RECOMMENDATIONS

A consistent P_1 solution scheme has been formulated and numerically implemented into the DOT IV computer program to obtain approximate solutions of the multigroup two-dimensional transport equation. The implementation represents a first attempt at obtaining P_1 solutions via DOT IV and in no way attempts to incorporate all the optional features of the code. The formulation was suggested by Carlson and is similar, if not equivalent, to Schmidt's method. Test problems were analyzed to determine the utility as well as the limitations of the method.

The iterative scheme employed was similar to the Peaceman-Rachford alternating direction implicit iteration scheme.[8] The Peaceman-Rachford scheme employs an acceleration parameter which serves to speed the convergence of the iterative process. It was found that the convergence rate of the consistent P_1 solution scheme is comparable to an unaccelerated Peaceman-Rachford iteration for certain problems. Diffusion theory matrices are S-matrices[7] and much can be said regarding this. One important note is that the spectral radius is less than unity and therefore the iterative process will converge. To derive equations which are stable with respect to round off errors, auxiliary functions were introduced in the P_1 formulation. This resulted in nonlinear recursion equations for the unknown functions. Efforts to write the P_1 difference

equations in matrix form were consequently unsuccessful and no conclusions could be reached regarding convergence.

The P_1 solution scheme was shown to agree with diffusion theory for problems having isotropic scattering and no anisotropic source. The diffusion routines exhibit a faster convergence and are therefore superior for problems of this nature. For problems with anisotropic scattering or sources, a full P_1 solution is superior.

Although the P_1 solution scheme implemented in DOT IV does have the capability of solving boundary source problems, the limitations and disadvantages of the current scheme are such that it should be discarded in favor of a better scheme. A major purpose of diffusion and P_1 approximations are to provide reasonable estimates for preliminary design calculations. Since a sufficiently fine mesh is required in general and no acceleration of the iterative process has been successful, the cost of obtaining a preliminary calculation may indeed be greater than that required to obtain a more accurate solution. However, if the convergence rate could be accelerated and thus make the method of practical value, the method could offer an attractive alternative to diffusion solutions by providing more accurate results as illustrated by the hydrogenous medium test case.

It is recommended that a further study of the mathematical properties of the resultant finite difference equations in matrix form be made to investigate the possibility of accelerating the convergence of the iterative scheme.

LIST OF REFERENCES

LIST OF REFERENCES

1. Lathrop, K. D., "Discrete-Ordinates Methods for the Numerical Solution of the Transport Equation," Reactor Technology, 15: 107-133 (1972).

2. Rhoades, W. A. and F. R. Mynatt, "The DOT III Two-Dimensional Discrete Ordinates Transport Code," ORNL-TM-4280, Oak Ridge National Laboratory (September 1973).

3. Rhoades, W. A., "The DOT IV Two-Dimensional Discrete Ordinates Transport Code," ORNL-5283, Oak Ridge National Laboratory (in preparation).

4. Lee, C. E., "The Discrete S_N Approximation to Transport Theory," LA-2595, Los Alamos Scientific Laboratory (March 1962).

5. Carlson, B. G. and K. D. Lathrop, "Transport Theory-The Method of Discrete Ordinates," LA-3251-MS(revised), Los Alamos Scientific Laboratory (October 1965).

6. Bell, G. I. and S. Glasstone, Nuclear Reactor Theory, New York, New York: Van Nostrand Reinhold Company, 1970.

7. Wachspress, E. L., Iterative Solutions of Elliptic Systems and Applications to the Neutron Diffusion Equations of Reactor Physics, Englewood Cliffs, New Jersey: Prentice Hall, Inc., 1966.

8. Greenspan, H., C. N. Kelber, and D. Okrent (Eds.), Computing Methods in Reactor Physics, New York, New York: Gordon and Breach Science Publishers, 1968.

9. Reed, W. H., "Spherical Harmonic Solutions of the Neutron Transport Equation from Discrete Ordinate Codes," Nuclear Science and Engineering, 49: 10-19 (September 1972).

10. Hansen, G. E. and W. H. Roach, "Six and Sixteen Group Cross Sections for Fast and Intermediate Assemblies," LAMS-2543, Los Alamos Scientific Laboratory (December 1961).

11. Courant, R. and D. Hilbert, Methods of Mathematical Physics, Vol. I, New York, New York: Interscience Publishers, Inc., 1953.

APPENDIX

APPENDIX

CONSISTENT P_1 APPROXIMATION

The P_1 approximation to the angular flux, independent of geometry, was given by

$$\Phi(\vec{r},\vec{\Omega},E) = \frac{1}{4\pi}\,[\phi(\vec{r},E) + 3\vec{\Omega}\cdot\vec{J}(\vec{r},E)]. \tag{A.1}$$

It will be the objective of this appendix to prove the validity of Equation (A.1) by expanding the angular flux in a truncated series of spherical harmonics.

Since the angular flux, together with its derivatives up to second-order, is continuous, it may be expanded in a series of spherical harmonics. If the direction vector is specified by a polar angle, θ, and an azimuthal angle, ϕ, then the expansion may be written

$$\Phi(\vec{r},\vec{\Omega},E) = \sum_{\ell=0}^{\infty}\sum_{m=0}^{\ell}\{a_{\ell,m}(\vec{r},E)\,P_\ell^m(\mu)\cos m\phi + b_{\ell,m}(\vec{r},E)P_\ell^m(\mu)\sin m\phi\}, \tag{A.2}$$

where $P_\ell^m(\mu)$ are associated Legendre functions given by

$$P_\ell^m(\mu) = [1-\mu^2]^{m/2}\,\frac{d^m P_\ell(\mu)}{d\mu^m}, \tag{A.3}$$

with $m = 0, 1, \ldots, \ell$ and $\mu = \cos\theta$. With the standardization $P_o(\mu) = 1$, the Legendre polynomials are found using

$$P_\ell(\mu) = \frac{1}{2^\ell \ell!}\,\frac{d^\ell}{d\mu^\ell}\,(\mu^2-1)^\ell. \tag{A.4}$$

The series represented by Equation (A.2) is absolutely and uniformly convergent.[11]

Neglecting terms having ℓ greater than one, expansion of Equation (A.2) yields, after simplification,

$$\Phi(\vec{r},\vec{\Omega},E) = A + B\mu + C\sqrt{1-\mu^2}\cos\phi + D\sqrt{1-\mu^2}\sin\phi. \tag{A.5}$$

To find each unknown, Equation (A.5) is multiplied by the coefficient for that unknown and then integrated over μ and ϕ. Performing these operations gives, after simplification,

$$\Phi = \frac{1}{4\pi}\{\phi+3[\mu\int_{\vec{\Omega}}\mu\Phi d\vec{\Omega} + \sqrt{1-\mu^2}\cos\phi\int_{\vec{\Omega}}\sqrt{1-\mu^2}\cos\phi\Phi d\vec{\Omega}$$

$$+\sqrt{1-\mu^2}\sin\phi\int_{\vec{\Omega}}\sqrt{1-\mu^2}\sin\phi\Phi d\vec{\Omega}]\}. \tag{A.6}$$

As given in Figure 1, page 7 or Figure 2, page 8, each coefficient of the integrals within brackets is a component of $\vec{\Omega}$. The integrals themselves are, by definition, components of the current. With these observations, Equation (A.6) may be written

$$\Phi(\vec{r},\vec{\Omega},E) = \frac{1}{4\pi}[\phi(\vec{r},E) + 3\vec{\Omega}\cdot\vec{J}(\vec{r},E)].$$

VITA

David Bruce Simpson was born in Knoxville, Tennessee on May 1, 1949. He was graduated from Central High School in that city in 1967. While an undergraduate at The University of Tennessee, he was a member of the Cooperative Engineering Program, and he received a Bachelor of Science degree in Nuclear Engineering in June 1972. Upon graduation, he accepted employment as a research assistant in the College of Engineering at The University of Tennessee and began study toward a Master of Science degree. He accepted employment with Oak Ridge National Laboratory in February 1974 and received his Master's degree in June 1977.

He is married to the former Anna Darlene Clark of Knoxville, Tennessee. They have one son, Brian Alan, born in May 1976.